7134–7146 *Nucleic Acids Research, 2011, Vol. 39, No. 16* *Published online 20 May 2011*
doi:10.1093/nar/gkr376

Adenine and guanine recognition of stop codon is mediated by different N domain conformations of translation termination factor eRF1

Konstantin N. Bulygin[1], Yulia S. Khairulina[1], Petr M. Kolosov[2], Aliya G. Ven'yaminova[1], Dmitri M. Graifer[1], Yuri N. Vorobjev[1], Ludmila Yu. Frolova[2] and Galina G. Karpova[1,*]

[1]Institute of Chemical Biology and Fundamental Medicine, Siberian Branch of the Russian Academy of Sciences, Novosibirsk, 630090 and [2]Engelhardt Institute of Molecular Biology, the Russian Academy of Sciences, Moscow, 119991, Russia

Received February 25, 2011; Revised and Accepted April 29, 2011

ABSTRACT

Positioning of release factor eRF1 toward adenines and the ribose-phosphate backbone of the UAAA stop signal in the ribosomal decoding site was studied using messenger RNA (mRNA) analogs containing stop signal UAA/UAAA and a photoactivatable cross-linker at definite locations. The human eRF1 peptides cross-linked to these analogs were identified. Cross-linkers on the adenines at the 2nd, 3rd or 4th position modified eRF1 near the conserved YxCxxxF loop (positions 125–131 in the N domain), but cross-linker at the 4th position mainly modified the tripeptide 26-AAR-28. This tripeptide cross-linked also with derivatized 3′-phosphate of UAA, while the same cross-linker at the 3′-phosphate of UAAA modified both the 26–28 and 67–73 fragments. A comparison of the results with those obtained earlier with mRNA analogs bearing a similar cross-linker at the guanines indicates that positioning of eRF1 toward adenines and guanines of stop signals in the 80S termination complex is different. Molecular modeling of eRF1 in the 80S termination complex showed that eRF1 fragments neighboring guanines and adenines of stop signals are compatible with different N domain conformations of eRF1. These conformations vary by positioning of stop signal purines toward the universally conserved dipeptide 31-GT-32, which neighbors guanines but is oriented more distantly from adenines.

INTRODUCTION

Elongation of the polypeptide chain of a protein that is synthesized on the ribosome terminates when one of three nonsense, or stop codons of the messenger RNA (mRNA), UAA, UGA or UAG, appears at the ribosomal A-site instead of sense codons encoding for amino acids. Thus, termination of polypeptide synthesis is one of the key steps of translation: it ensures formation of the normally sized proteins. Stop codons are decoded at the ribosome by polypeptide chain release factors class 1 (RF1/RF2 in bacteria or eRF1 in eukaryotes) that are responsible for the recognition of the A-site-bound stop codons and triggering hydrolysis of the complex ester bond between the peptidyl moiety and the 3′-terminal ribose of the P-site-bound peptidyl-transfer RNA (tRNA) at the ribosomal peptidyl transferase center (1–3). The process also involves termination factor class 2 (RF3 in bacteria or eRF3 in eukaryotes), eRF3 is the ribosome- and eRF1-dependent GTPase (4). RF3 is essential for dissociation of RF1/RF2 from the ribosome after termination (5) while eRF3 ensures rapid and efficient hydrolysis of peptidyl-tRNA (6). Moreover, eRF3 stimulates release activity of eRF1 (4,6,7), with which it can form a stable complex (8–11). Although steps of translation termination in bacteria and eukaryotes share considerable similarity, bacterial and eukaryotic class 1 RFs do not possess any obvious sequence homology (3,12,13) and there are numerous indications that molecular mechanisms of termination on 70S and 80S ribosomes are different (14). Structural aspects of the interaction of bacterial RF1/RF2 with the ribosome and mechanisms of stop codon recognition by these factors are well studied, in

*To whom correspondence should be addressed. Tel: +7(383) 363 5140; Fax: +7(383) 363-5153; Email: karpova@niboch.nsc.ru
Correspondence may also be addressed to Ludmila Yu. Frolova. Tel: +7(495) 135 9986; Fax: +7(495) 135 1405; Email: frolova@eimb.ru

The authors wish it to be known that, in their opinion, the first two authors should be regarded as joint First Authors.

particular due to a remarkable progress in X-ray crystallography and cryo-electron microscopy (15–17). The crystal structures of eRF1 in solution (18) as well as the ribosome-free complexes of eRF1 with eRF3 (19) have been solved. However, structural information on the positioning of eRF1 in the 80S termination complexes is limited since these complexes have not yet been studied by either cryo-electron microscopy or X-ray crystallography that has only recently been adapted to decipher the structure of ribosomes of lower eukaryotes (20,21).

The conventional point of view is that eRF1 has a tRNA-mimic structure, in which the universal GGQ motif located on the tip of the M domain of eRF1 and common to all class-1 RFs is equivalent to the acceptor end of tRNAs, while the conserved NIKS motif (positions 61–64 in human eRF1) recognizing the first uridine of the stop codon corresponds to the anticodon loop of tRNAs (3). In the three-dimensional structure of eRF1, the stop codon recognition site ('anticodon') is discontinuous and, besides the NIKS motif, includes the highly conserved YxCxxxF motif (positions 125–131) involved in the recognition of purines (19,22,23). Apparently, eRF1 cannot be positioned in the ribosomal A-site in the form known from X-ray crystallographic studies (18) since the distance between the GGQ and NIKS motifs in eRF1 is about 100 Å that is much larger than the distance between the acceptor end and the anticodon loop in a tRNA (typically, 75–80 Å). This implies that eRF1 can be adopted at the ribosomal A-site only when it undergoes major conformational rearrangements. Such rearrangements have been observed in the X-ray crystallographic studies of eRF1 complexed with eRF3 (19) and modeled (24).

It is clear that information on the positioning of eRF1 with respect to the components of 80S translation termination complexes is essential to understand molecular mechanisms of translation termination in eukaryotes. Data on the eukaryotic stop codon recognition site have mainly been obtained by investigating the effects of mutations in designed regions of eRF1 on recognition of particular stop codons and do not provide direct information on positioning of eRF1 with respect to the A-site-bound stop codon in the 80S termination complex (22,23,25–30). This information has been obtained partially from X-ray studies of the eRF1•eRF3 complex containing a bound ATP molecule that mimicked a nucleotide of stop codon according to authors' suggestion (19), and from results on site-directed cross-linking of the A-site-bound stop codon to eRF1 in the 80S ribosomal termination complexes (24,31). It is evident that the data for ribosome-free eRF1•eRF3•ATP complexes (19) cannot adequately reflect positioning of a stop codon in the 80S termination complex in contrast to cross-linking data. The use of a set of mRNA analogs with perfluorophenyl azide-derivatized guanines made it possible to identify the conserved N domain YxCxxxF and the GTx motifs as neighbors of the guanine of the A-site-bound UGA and UAG stop codons (24). However, positioning of eRF1 with respect to the adenines of stop codons in the 80S termination complexes remained to be studied. For this reason, in the current study we examined positioning of the adenines of the UAAA terminating tetraplet with respect to eRF1 in the 80S termination complexes using mRNA analogs bearing UAA or UAAA at the 3′-end and the perfluorophenyl azide cross-linker at the C8 of the adenosine or at the 3′-terminal phosphate. Identification of the peptides cross-linked to nucleotides of the stop signal and comparison of the results obtained with data on molecular modeling of eRF1 fitted to the A-site adjacent to the P-site-bound tRNA makes it possible to conclude that eRF1 adopts different conformations of its N domain to recognize adenines and guanines of stop codons.

MATERIALS AND METHODS

$tRNA^{Phe}$ (1300 pmol/A_{260} unit) was a kind gift from Dr. V. Katunin (Konstantinov's St. Petersburg Institute of Nuclear Physics, Gatchina, Russia). Isolation of the 40S and 60S ribosomal subunits from unfrozen human placenta and their association in 80S ribosomes were performed as described (32). The activity of the ribosomes in the poly(U)-directed binding of [^{14}C]Phe-$tRNA^{Phe}$ was ~70% (extent of binding was about 1.4 mol of Phe-$tRNA^{Phe}$ per mole of the 80S ribosomes at saturating concentration of Phe-$tRNA^{Phe}$).

mRNA analogs

Synthesis and purification of derivatives of oligoribonucleotides bearing an 4-azido-2,3,5,6-tetrafluorobenzoyl group attached via specific spacers to either the 3′-terminal phosphate or the C8 of the adenine were carried out as described in refs. 33 and 34, respectively. Before use in the cross-linking experiments, the derivatives were 5′-^{32}P-labeled and purified (35).

eRF1

DNA constructions for the preparation of recombinant human eRF1 and its mutants with a C-terminal His-tag were described (23,31,36). The eRF1 proteins were expressed in *Escherichia coli* and purified by affinity chromatography as described (37). The eRF1 activity was measured *in vitro* as described (38,39).

Ribosomal complexes and cross-linking procedures

Complexes of 80S ribosomes (5.0×10^{-7} M) with $tRNA^{Phe}$ (5×10^{-6} M) and mRNA analogs (3.5×10^{-6} M) were obtained by incubating these components for 40 min in buffer A [20 mM HEPES-KOH, pH 7.5, 100 mM NH_4Cl, 4 mM $MgCl_2$, 0.2 mM ethylenediaminetetraacetic acid (EDTA), 0.6 mM spermidine and 0.8 mM spermine] at room temperature. The reaction mixtures for cross-linking experiments contained 15 pmol of 80S ribosomes. Then wild-type (wt)-eRF1 or mutant eRF1 was added, where specified, in a 7-fold molar excess each over the 80S ribosomes and the reaction mixtures were further incubated for 40 min at room temperature. To obtain cross-links between mRNA analogs and eRF1, complexes were ultraviolet (UV)-irradiated as described (40). Reactions were stopped with 1/30 v/v of 5% 2-mercaptoethanol and the ribosomal complexes were purified by

centrifugation in a sucrose gradient (15–30%) containing buffer A with 1 mM 2-mercaptoethanol as described (33).

eRF1 mapping

Isolation of eRF1 (wild-type or mutant) cross-linked to a labeled mRNA analog in the termination complex, its CNBr-induced cleavage and separation of the resulting fragments were carried out as described (24). Selective cleavage of the labeled eRF1 fragments obtained as a result of CNBr-induced digestion of cross-linked eRF1 with the endoproteases GluC, ArgC (Roche), pepsin (Sigma-Aldrich) or with hydroxylamine and separation of the resulting fragments by 16.5% Tris–tricine sodium dodecyl sulfate–polyacrylamide gel electrophoresis (SDS–PAGE) were performed according to ref. 24; the gels were dried and radioautographed. Hydrolysis of cross-linked eRF1 oligopeptides corresponding to radioactive bands excised from the dried gels with endoprotease AspN (Roche) was carried out in 100 µl of 10 mM Tris–HCl buffer, pH 7.5, containing 0.001 µg/µl of the enzyme by incubating of mixture overnight at 37°C with subsequent analysis by Tris–tricine SDS–PAGE as described.

RESULTS

mRNA analogs

The mRNA analogs contained the Phe codon UUC followed either by the UAA(p) triplet or the UAAA(p) tetraplet and carried a perfluorophenyl azide group attached via a spacer to the C8 atom of the adenine or to the 3′-terminal phosphate (Figure 1A). mRNA analogs containing sense codons (pUUCUA*CAAA, pUUCUC A*AAA, and pUUCUCAp*) were used in control experiments. The position of the modified nucleotide varied from the second to the fourth position in the termination tetraplet. The UUC codon of the mRNA analogs was targeted to the ribosomal P site by $tRNA^{Phe}$ so that the adjacent modified stop codon was directed to the A site (Figure 1B). This complex is referred as a 'phased' ribosome.

Cross-linking of mRNA analogs to the components of the ribosomal complexes

Complexes of 80S ribosomes with mRNA analogs and $tRNA^{Phe}$ obtained in the presence of eRF1 were irradiated and then purified to remove eRF1 that could be cross-linked to mRNA analogs outside of the ribosome (24). The results of cross-linking of mRNA analogs (Figure 1A) to ribosomal proteins and eRF1 presented in Figure 2 are similar to those obtained recently with the use of similar mRNA analogs with derivatized guanines (24). In particular, the addition of $tRNA^{Phe}$ to mixtures of ribosomes with mRNA analogs results in significant enhancement of cross-linking to some ribosomal proteins (Figure 2, compare lanes 1 with other lanes). Protein bands in the upper and middle parts of the gels correspond to cross-linked proteins S2/S3 and S15, respectively. This assignment is based on our earlier studies where these proteins have been found to cross-link to mRNA analogs whose perluorophenyl azide-modified nucleotides were placed on the 80S ribosome in positions +4 to +7 with respect to the first nucleotide of the P-site-bound codon (40,41). Strong tRNA-dependent cross-linking to protein S15 has been shown to be characteristic for the modified nucleotides in mRNA positions from +4 to +7; in Figure 2, the respective bands are seen in lanes 2 and 3 with phased ribosomes but not in lanes 1 corresponding to complexes obtained without tRNA. In contrast, cross-linking to proteins S2/S3 slightly depends on the presence of tRNA (40,41); in Figure 2, the respective bands are seen in all lanes.

The addition of eRF1 to the phased ribosomes with subsequent irradiation causes appearance of a new radioactive band in the upper part of the gels (Figure 2, lanes 3) whose mobility corresponds to that of eRF1 (Figure 2, lanes 4). This cross-linking to eRF1 is specific for the mRNA analogs containing stop codon UAA since mRNA analogs bearing UAC or UCA sense codon with modified adenosine or 3′-terminal phosphate cross-link to eRF1 negligibly (Figure 2, lanes 5). The yield of the cross-link eRF1-mRNA analog depends both on the position of modified nucleotide and on the site of the cross-linker in it. The lowest yield is observed with mRNAs I and II bearing a modified A in the second and third stop codon positions, respectively (Figure 2).

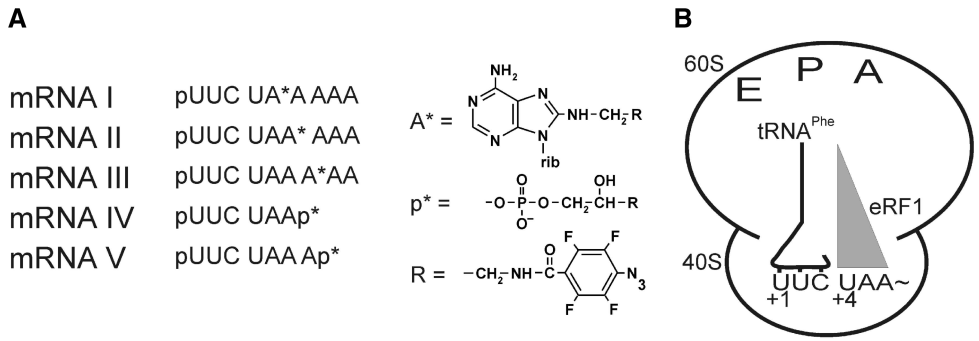

Figure 1. mRNA analogs and ribosomal complexes. (**A**) mRNA analogs used here. (**B**) 80S ribosome complexed with an mRNA analog, tRNA and polypeptide chain release factor eRF1. The distance separating the modified adenine base (or the 3′-phosphate) and the first nitrogen of the azidogroup is ≤11 Å.

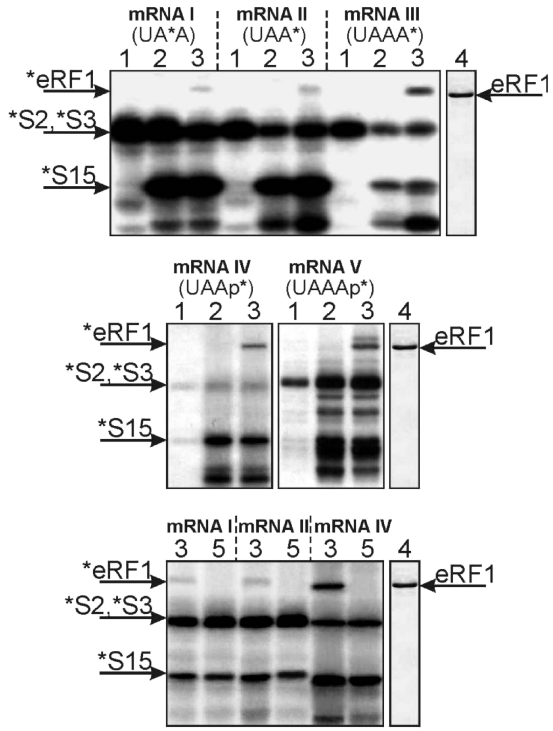

Figure 2. Electrophoretic analyses of irradiated ribosomal complexes. Autoradiogram of SDS–PAGE. Upper parts of the gels with rRNA bands are not shown. Complexes are numbered according to the lane numbers (indicated above the autoradiograms). 80S•mRNA (1), 80S•mRNA•$tRNA^{Phe}$ (2), 80S•mRNA•$tRNA^{Phe}$•eRF1 (3). Lane 4, stained electrophoregrams of eRF1. Lane 5, complexes 80S•mRNA (sense)•$tRNA^{Phe}$ obtained in the presence of eRF1 with the use of mRNA analogs pUUCUA*CAAA, pUUCUCA*AAA and pUUCUCAp* instead of mRNAs I, II and IV, respectively. Bands corresponding to cross-linked eRF1 and ribosomal proteins (marked with asterisks) are indicated by arrows.

Initial analysis of the cross-linking sites on the eRF1 protein by CNBr-induced cleavage

The strategy used for the initial mapping of the cross-linking sites on the eRF1 was based on the specific CNBr-induced complete cleavage of eRF1 after methionine residues with subsequent SDS–PAGE analysis of the resulting fragments (24). The data presented in Figure 3 show that all lanes share a band marked '**a**' corresponding to the products whose masses after subtracting the masses of the cross-linked mRNA analogs (ranging from 2.2 to 3.2 kDa) were ~16 kDa (Figure 3A). This band can be unambiguously assigned to the cross-linked 52–195 fragment of eRF1 (Figure 3B). With mRNAs III, IV and V, one can observe the faster migrating band b together with band a (Figure 3A, lanes 3–5), and the relative intensities of these bands depend on the site of the cross-linker in the mRNA analog. Thus, band **b** is much stronger than band **a** in the case of mRNA III (Figure 3A, lane 3), while with mRNA V band **a** is stronger (Figure 3A, lane 5). In experiments with mRNA IV, practically only band **b** is observed (Figure 3A, lane 4).

Mapping of the cross-linking sites corresponding to band 'a'

To precisely identify the positions of the cross-links in the 52–195 fragment, the strategy applied earlier for guanosine-derivatized mRNA analogs was used (24). To examine cross-linking of mRNAs I–III in the region of the YxCxxxF motif, which was one of the targets for cross-linking in the above-mentioned study, eRF1 mutants with double amino acid substitutions were used. One out of two substitutions eliminated the CNBr cleavage site in the wt-eRF1 that borders the 51–195 fragment (M195L or M51A), and another substitution inserted a new artificial site for CNBr cleavage absent in the wt-eRF1 near or within the YxCxxxF motif (K109M, I120M, L124M, L126M or H132M). The results of the SDS–PAGE analysis of cross-linked products obtained with the eRF1 mutants are presented in Figure 4. With the mRNA analogs I–III, the labeled products corresponding to the upper bands migrate more slowly with the mutant K109M + M195L than with I120M + M195L (Figure 4A, left panel, lanes 2 and 3). This is possible only if the cross-linking sites are in the fragments 110–241 and 121–241, respectively (Figure 4B, lanes 2 and 3), restricting location of the cross-links within positions 121–195 with all mRNA analogs. The data obtained with the remaining eRF1 mutants are presented in Figure 4A (right panel). A comparison of the mobilities of the products corresponding to the upper bands (Figure 4A, lanes 4–6 with mRNA I) with the cleavage map presented in Figure 4B shows that with mRNA I cross-linked fragments can only be aa 125–195, 127–195 and 35–132; therefore, the cross-link is in positions 127–132. Similarly, the data obtained with mRNA III clearly imply that the cross-linked fragments are aa 35–124, 35–126 and 35–132 (compare lanes 4, 5 and 6 with mRNA III in Figure 4A and B). Taking into account that all mRNAs I–III cross-links corresponding to the upper bands are in positions 121–195, one can conclude that the site of mRNA III cross-linking lies within positions 121–124. Finally, with mRNA II two cross-linking sites exist, in positions 121–124 and 125–132 (Figure 4A and B, lanes 4–6).

As for mRNA IV, the mapping has not been carried out since with the above-mentioned mutants yield of cross-linking corresponding to band **a** is too low (Figure 3, lane 4). In the experiments with the mutants and mRNA V, the position of band **a** is the same as with the wt-eRF1 (data not shown). Thus, in this case the cross-linking site is outside from the YxCxxxF region. To map the cross-link with mRNA V, a set of eRF1 mutants carrying single amino acid substitutions for Met in another putative region of the 52–195 fragment was used, namely, the region of the NIKS motif (fragment 61–64). These mutants were previously used to identify the eRF1 fragment cross-linked to the first nucleotide of a stop codon (24,31). The results presented in Figure 5 clearly show that with mutant V66M the cross-linked fragment is slightly shorter than with wt-eRF1, while with mutant G73M it is drastically shorter (lanes 2 and 3). These data imply that the respective cross-linked fragments are aa 67–195 and 52–73, respectively (Figure 5B, compare lanes 2

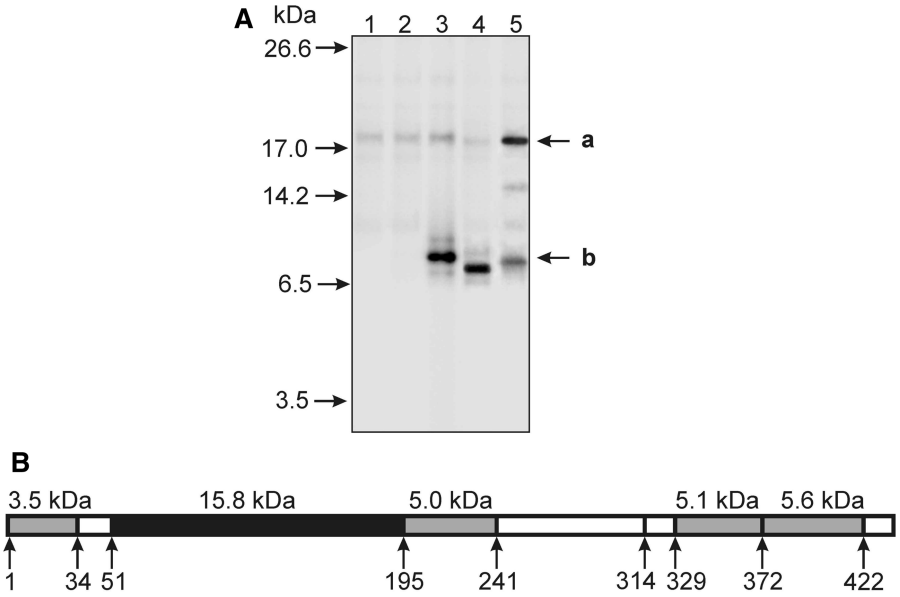

Figure 3. Mapping of cross-linking site(s) in human eRF1. (**A**) Autoradiogram. SDS–PAGE analysis of the fragments resulting from the CNBr-induced cleavage of eRF1 cross-linked to end-labeled mRNA analogs. Lane numbers correspond to the numbers of mRNA analogs (Figure 1). Positions of bands corresponding to molecular mass markers are given on the left. (**B**) Schematic representation of the CNBr-induced cleavage sites of human eRF1 (437 aa long), calculated masses of the fragments in kilo daltons are indicated above the diagram. The fragment corresponding to band **a** is highlighted in black; candidate fragments for band **b** are presented in gray.

and 3 to lane 1), and therefore the cross-link falls in positions 67–73.

Mapping of the cross-linking sites corresponding to bands 'b'

The electrophoretic mobilities of products corresponding to bands **b** with mRNAs III–V are somewhat different, but these differences evidently relate to the masses of the mRNA analogs cross-linked to oligopeptides rather than with masses of the oligopeptides subjected to the cross-linking. The most slowly migrating product is observed with mRNA III (a nonamer), the fastest is obtained with mRNA IV (a hexamer) and the oligopeptide cross-linked to mRNA V (a heptamer) has an intermediate mobility. The apparent masses of the oligopeptides after subtracting the masses of the cross-linked mRNA analogs are in the range of 4–5 kDa. However, the molecular mass of the cross-linked product migrating as band **b** could be not exactly the same as expected from its electrophoretic mobility due to influence of the cross-linked oligonucleotide moiety on the mobility of the modified oligopeptide in the gel. The shorter the oligopeptide is, the more effect of the cross-linked oligonucleotide is expected. Therefore, bands **b** observed with mRNAs III–V can correspond to any of four candidate fragments 2–34, 196–241, 330–372 and 373–422 whose molecular masses are rather close to the expected range of 4–5 kDa (Figure 3B). Cross-linking within the fragment 196–241 is excluded based on the results obtained with mutants K109M + M195L and I120M + M195L (see above) since CNBr-induced cleavage of these mutants cross-linked to mRNA III produced the same bands **b** as wt-eRF1 (Figure 4A, left panel; data with mRNAs IV and V are similar and are not shown). Cross-linking within the fragment 373–422 is excluded based on analogous results with eRF1 mutants carrying single substitutions of amino acids for Met in this region (data not shown). To distinguish between the remaining candidate fragments 2–34 and 330–372, we conducted cleavage of cross-linked peptide with various proteolytic agents with subsequent analysis of the resulting products by Tris–tricine SDS–PAGE. Identification of short oligopeptides cross-linked to each mRNA analog was based on comparison of relative positions of the bands obtained with the respective proteolytic agents with the map of eRF1 cleavage. The treatment of cross-linked oligopeptide with an agent should result in the changes of the respective SDS–PAGE pattern if the oligopeptide contains site(s) for cleavage with this agent; moreover, faster migrating band corresponds to shorter oligopeptide cross-linked to the mRNA analog. So, we treated bands **b** excised from the gels with endoprotease ArgC, which has cleavage sites in fragment 2–34 but not in fragment 330–372 (except for Arg330). With all mRNAs III–V, the product corresponding to band **b** is sensitive to ArgC implying that the cross-links are in positions 2–34 (Figure 6A, compare lanes 1 and 3).

To refine the cross-link positions within the 2–34 fragment, the products corresponding to bands **b** were cleaved with hydroxylamine, endoprotease ArgC or endoprotease GluC (Figure 6, lanes 2–4). Treatment with hydroxylamine causes slight but visible shift of bands **b** indicating that the hydrolysis shortens the oligopeptide slightly and therefore excludes cross-link in positions 31–34 (Figure 6, lanes 2). In all cases, the products resulting from treatment with ArgC (lanes 3, bands **c**) migrate much more slowly than the fragment after the GluC

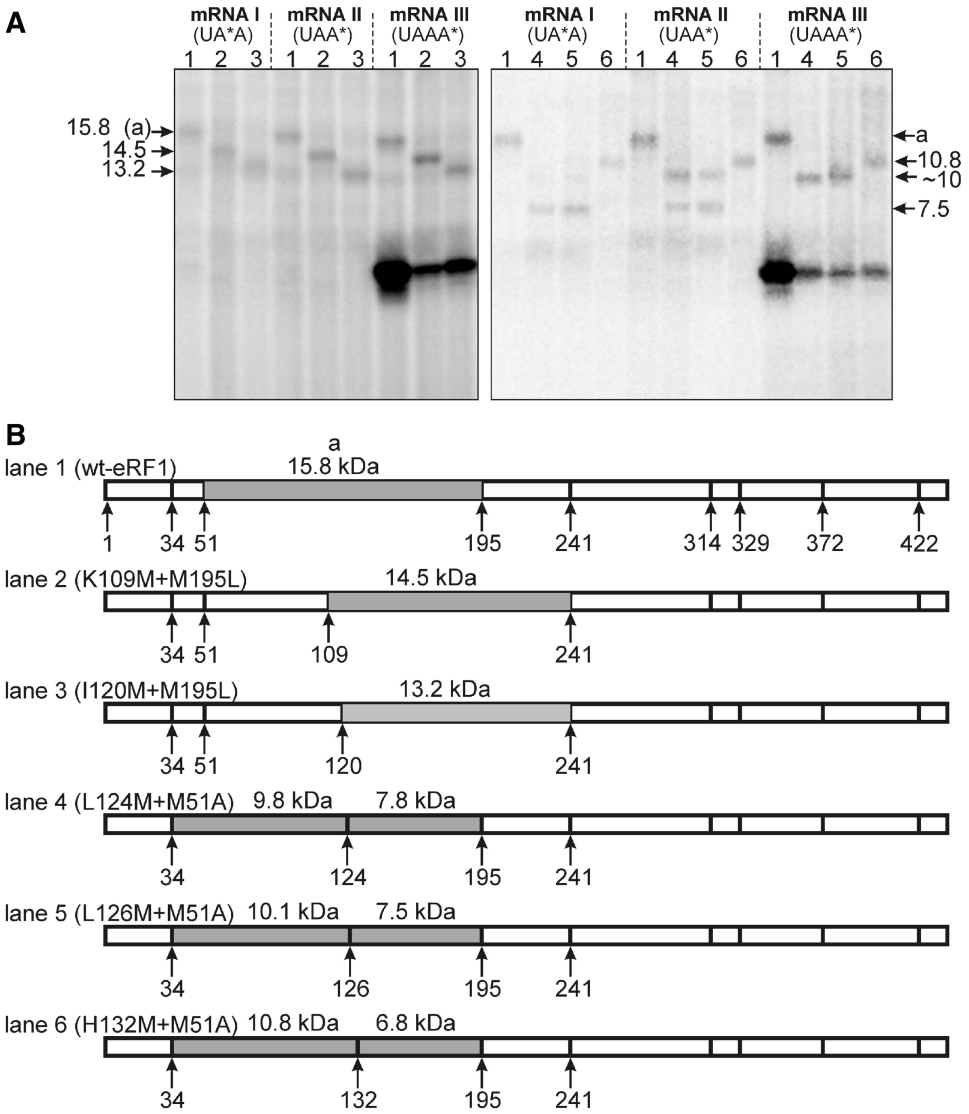

Figure 4. Mapping of the cross-linking sites within the region 52–195 using double eRF1 mutants. (**A**) Autoradiograms. Patterns of CNBr-induced cleavage fragments are obtained with two sets of double mutants (each set on a separate panel) cross-linked to mRNA analogs. Band **a** is marked by analogy with Figure 3. The expected molecular masses (kDa) of the labeled products resulting from the CNBr-induced cleavage positions are given on the sides of the panels (molecular masses of the cross-linked mRNA analogs were subtracted). (**B**) Schematic representations of the cleavage sites together with calculated molecular masses (kDa) of the fragments resulting from the CNBr-induced cleavage. Cross-linked fragments are presented as gray.

treatment (bands **d**) (compare lanes 3 and 4). This implies that ArgC produces the cross-linked 11–28 fragment since only in this case the cross-linked fragment obtained with ArgC should be larger than any labeled fragment resulting from GluC treatment (Figure 6B, lanes 3 and 4). To identify more precisely positions of the cross-links within fragment 11–28, we excised bands corresponding to labeled products of bands **b** digested with GluC (namely, bands **d**), and treated them with hydroxylamine, or pepsin or endoprotease AspN (Figure 6A, lanes 5–7 and Figure 6C). Among three possible fragments resulting after GluC treatment only the 26–34 fragment contains a site for cleavage with hydroxylamine (Figure 6B, lane 4, and Figure 6C, lane 5). Evidently, the product corresponding to band **d** (Figure 6A, lanes 4) is sensitive to hydroxylamine treatment, which leads to the formation of a faster migrating product, band **e**, with all mRNAs (Figure 6A, lanes 5). Consequently, bands **d** correspond to the cross-linked 26–34 fragment. This identification is confirmed by the results presented in Figure 6C (lanes 6 and 7) showing that the product corresponding to band **d** is insensitive both to pepsin and to endoprotease AspN. Indeed, of three candidate fragments that can correspond to bands **d** (aa 2–13, 14–25 or 26–34) only the 26–34 fragment does not contain cleavage sites for AspN and pepsin. Thus, the sites of mRNAs III–V cross-links are mapped to fragment 26–28.

Data on cross-linking of mRNA analogs to eRF1 are summarized in Table 1. It is clear that modified adenosines in the second and third positions of a stop codon

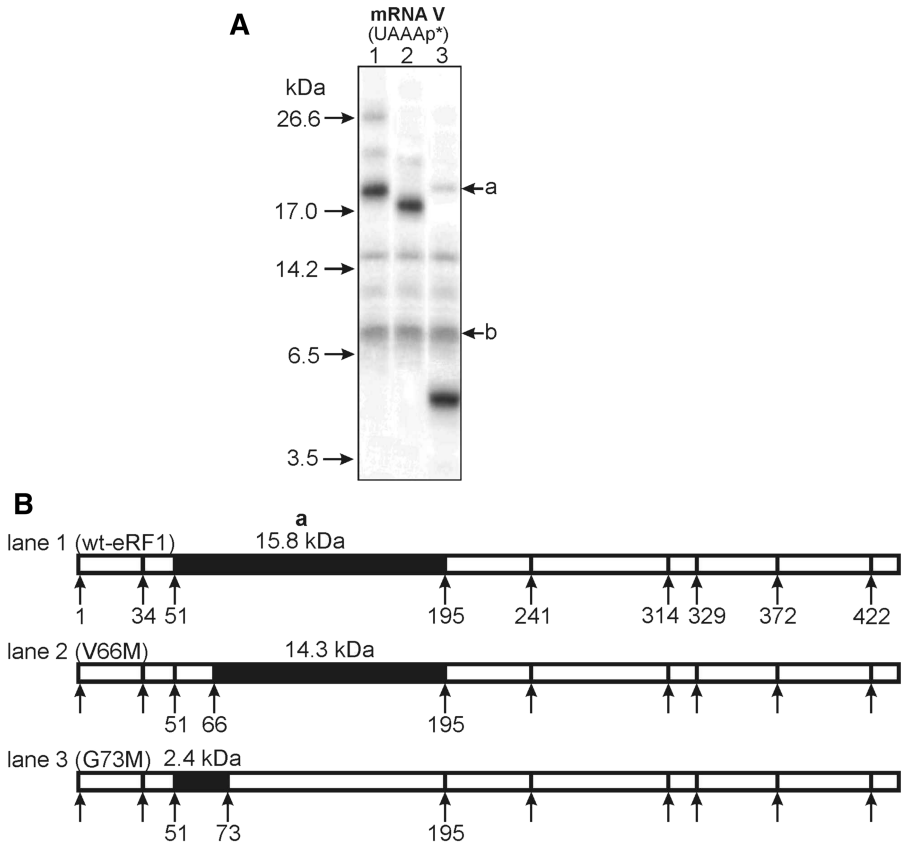

Figure 5. Mapping of the cross-linking site corresponding to fragment **a** within the 60–73 region using eRF1 mutants. (**A**) Patterns of CNBr-induced cleavage fragments obtained with eRF1 mutants cross-linked to mRNA analogs. Bands **a** and **b** are marked by analogy with Figure 3. (**B**) Schematic representation of the cleavage sites. Cross-linked fragments are highlighted in black.

cross-link only to the YxCxxxF region (aa 121–132). This cross-link becomes minor when the same nucleotide is in the fourth position of the termination tetraplet where it cross-reacts mainly with the 26–28 fragment. The latter site is practically the only one when the cross-linker is at the 3′-phosphate of the UAA stop codon. Cross-linking to this site is strongly reduced if the same group is at the 3′-phosphate of the UAAA tetraplet, which cross-links more strongly to the NIKS region.

A model for positioning of the UAA stop codon with respect to eRF1 in the termination complex

In a previous study (24), we described two alternative models of the eRF1 structure in the 80S termination complex obtained by molecular modeling based on the crystal structure of eRF1 and the available structural and functional information related to positioning of eRF1 toward the P-site-bound tRNA and the stop codon in the ribosome. Briefly, the structure of eRF1 was initially altered to fit optimally to the ribosomal A-site cavity. In particular, Y-shaped form of the eRF1 was transformed into a structure with a distance between the NIKS and GGQ motifs close to the distance between the anticodon triplet and the CCA-end of tRNA. Then this eRF1 structure was docked at the A-site-bound stop codon using the ribosomal structure 1JGO and the following constraints: CCA-end of the P-site-bound tRNA should be located very close to the GGQ tripeptide of eRF1, and NIKS motif should neighbor the first uridine of stop codon. One of two obtained models [referred as M1 model in (24)] has been chosen as fitting well to the cross-linking data. In this model, the mRNA passes through the cavity at the surface of the N domain in a vicinity of the contact between the N and C domains of eRF1, which adopts an L-shape tRNA-like conformation. The distance between the NIKS loop and the GGQ triplet is equal to 76 Å, and the distance between the stop codon and the GGQ triplet is equal to 74 Å (exactly as between the anticodon triplet and 3′-terminal A in tRNA). In the present study, the model was somewhat updated, in particular, to bring the GGQ tripeptide of eRF1 in closer proximity to the CCA terminus of the P-site-bound tRNA at the peptidyl transferase center of the ribosome (Figure 7). In this refined model, the surroundings of the CCA terminus of the P-site-bound tRNA and the eRF1 nanopeptide HGRGGQSAL correspond to the RF1•tRNA•ribosome complex (accession code 2B64) with an accuracy of 1 Å. Here, we have used this model to identify the eRF1 amino acid residues that neighbor perfluorophenyl azides at the UAAA termination tetraplet of mRNA analogs in the 80S termination complexes (Table 2).

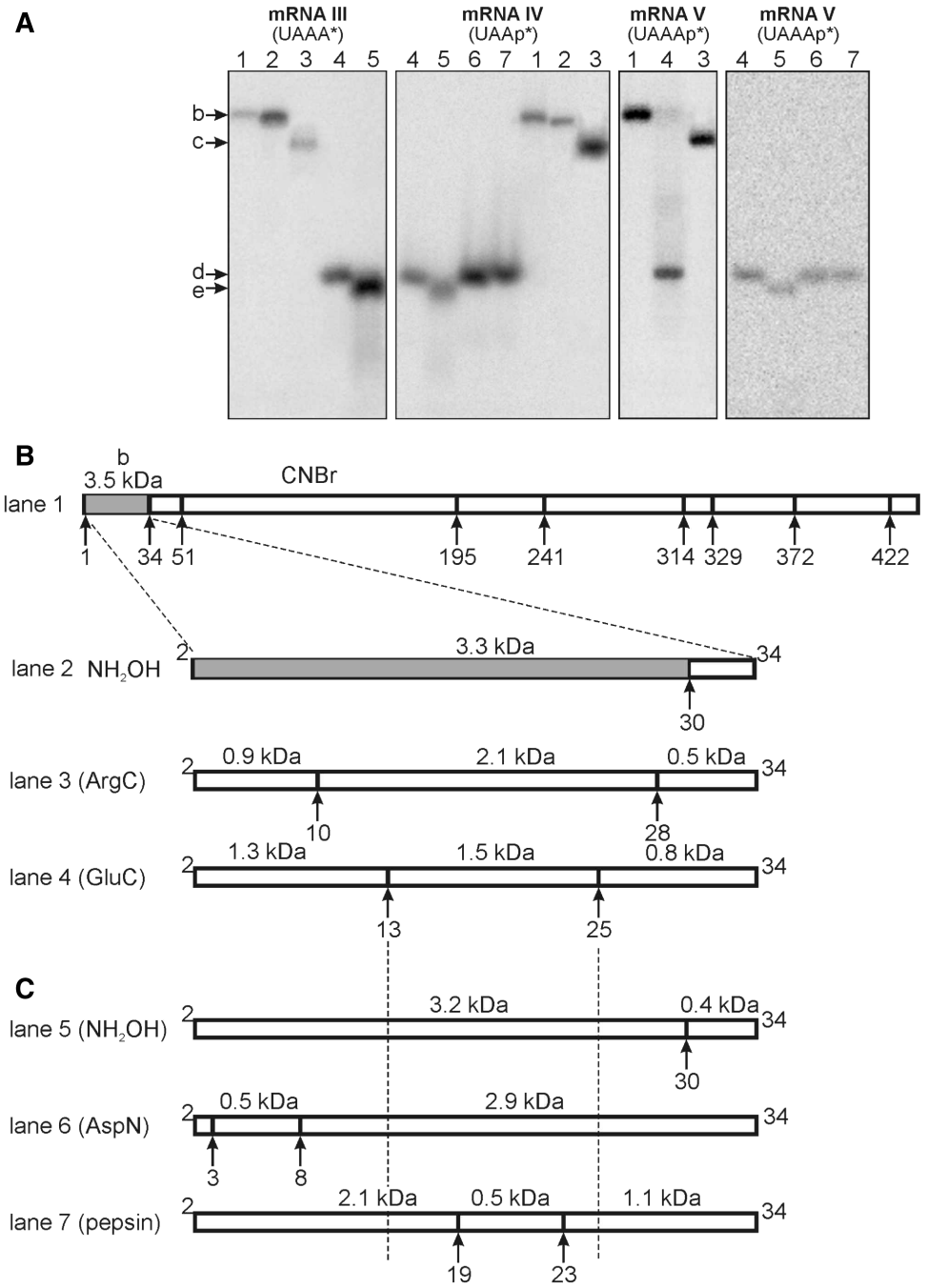

Figure 6. Mapping of the cross-linking site corresponding to fragment **b** within the 2–34 region. (**A**) Patterns of specific cleavage of the labeled product corresponding to band **b** (Figure 3) with hydroxylamine (lane 2) and endoproteases ArgC (lane 3) and GluC (lane 4). Lanes 5–7 correspond to treatment with hydroxylamine, endoprotease AspN or pepsin, respectively, of the labeled product **d** obtained as result of digestion of fragment b with endoprotease GluC (lane 4). The panels represent separate electrophoregrams that are artificially aligned to bring all the bands **b** at the same apparent migration positions. (**B**) Schematic representation of the CNBr-induced cleavage sites of human eRF1 and digestion of the 2–34 fragment with hydroxylamine and endoproteases ArgC and GluC. Fragments containing the cross-link are marked in gray. (**C**) Schematic representation of the cleavages of oligopeptides 2–13, 14–25 and 26–34 (shown with dotted vertical lines) in the 2–34 fragment with hydroxylamine, endoprotease AspN or pepsin.

It is noteworthy that in our model stop codon guanines are proximal to a fragment of the C domain of the eRF1 centered around aa 360, which is not expected from the X-ray structure of free eRF1 (18). But our model of the eRF1 structure in the 80S termination complex fits the nuclear magnetic resonance (NMR) data demonstrating that the C domain (minidomain 329–372) is located proximately to the N domain of human eRF1 (42), which may be considered as an additional validation of the model.

Table 1. Cross-linking sites of mRNA analogs on human eRF1

mRNA analog (Figure 1A)	Position of the modified nucleotide[b] and site of the cross-linker (shown in brackets)	Distribution of cross-links between fragments in the N-domain of eRF1[a]	
		Fragment 'a' (52–195)	Fragment 'b' (2–34)
I	+5 (A)	127–132 (100%)	No cross-links
II	+6 (A)	121–124, 125–132 (100%)	No cross-links
III	+7 (A)	121–124 (10%)	26–28 (90%)
IV	+6 (p)	Not identified	26–28 (>95%)
V	+7 (p)	67–73 (25%)	26–28 (75%)

[a]Quantified data from Figure 3A in percent of the total amount of cross-linked mRNA analog; relative error is ~10%.
[b]With respect to the 5′-terminal nucleotide of the mRNA analog (namely, to the first nucleotide of the UUC triplet targeted to the P site).

DISCUSSION

The use of short mRNA analogs bearing perfluorophenyl azide cross-linker at definite locations provides correct information on the immediate neighborhood of particular mRNA nucleotides in the eukaryotic ribosomal complexes. This conclusion is based on the comparison of the data on 18S rRNA nucleotides proximal to various mRNA positions obtained with these mRNA analogs (40,41) and with longer synthetic mRNAs bearing 4-thiouridine, a 'zero-length' cross-linker (24,43). Application of both types of mRNA analogs led to identification of very similar sets of 18S rRNA nucleotides neighboring mRNA in the 80S ribosomal complexes, despite different natures of the cross-linkers used and various ways of the formation of complexes. Locations of these 18S rRNA nucleotides in the conserved core of the small subunit rRNA secondary structure almost exactly corresponded to the locations of 16S rRNA nucleotides contacting the respective mRNA positions in the eubacterial 70S ribosomal complex (40,41), whose atomic structure is well known from X-ray crystallographic data. Thus, cross-links of perfluorophenyl azide-modified mRNA analogs to 18S rRNA actually reflected immediate neighborhood of the derivatized mRNA nucleotides in the eukaryotic ribosomal complexes, and needlessly to consider any of these cross-links as false ones. All these justify consideration of eRF1 peptides cross-linked to the mentioned mRNA analogs as actual nearest neighbors of the derivatized stop codon nucleotides in the 80S termination complexes.

The cross-linking results presented here indicate that adenines in the second and third positions of the UAA stop codon neighbor various parts of the region 125–131 containing the conserved YxCxxxF motif of human eRF1 (Table 1). Numerous data reported earlier indicate the involvement of this region in recognition and discrimination of stop codon purines (19,23,25,26,27). Amino acids of the YxCxxxF region of eRF1 have been found among the targets for cross-linking of mRNA analogs bearing a perfluorophenyl azide at the guanines in the UGA/UAG stop codons (24). These data together with the results of the present study show that amino acids of the YxCxxxF region neighbor purines of any stop codon in the 80S termination complex and imply that involvement of this region in recognition and/or discrimination of stop codon purines is most probably based on their direct interactions with YxCxxxF.

In this study, a novel site of cross-linking of mRNA analogs to eRF1, 26-AAR-28, is reported (Table 1).

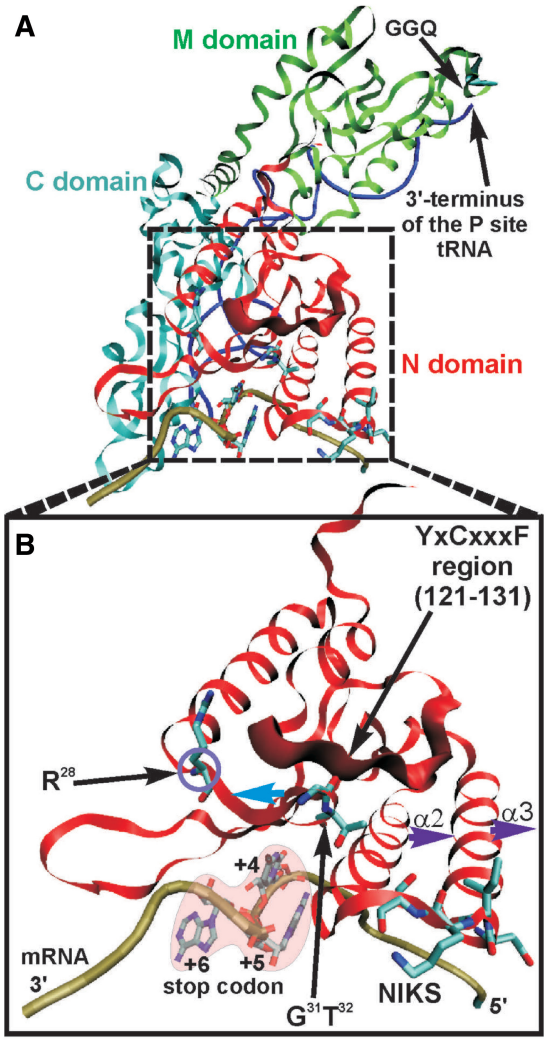

Figure 7. A model of positional relationship of mRNA, the P-site-bound $tRNA^{Phe}$ and the A-site-bound eRF1 in the 80S ribosomal termination complex. (**A**) General view. Phosphate backbone of the mRNA is presented as khaki tube; the P-site-bound $tRNA^{Phe}$ is given as dark blue tube; eRF1 is shown as ribbon (N domain is red, M domain is green and C domain is green-blue). (**B**) Zoomed detailed view of the part of the complex comprising the N domain of eRF1 and mRNA presented in the same way as in the general view. The NIKS region, the GT dipeptide in positions 31 and 32 of eRF1 and Arg28 are shown in the stick models (Arg28 is circled), YxCxxxF region (positions 121–131) is marked as wide ribbon; eRF1 helices α2 and α3 are indicated. Nucleotides of the A-site-bound stop codon (nucleotides in positions +4, +5 and +6 with respect to the first nucleotide of the P-site-bound codon) are shown in the stick models surrounded by a pink area. Arrows indicate suggested directions of movements of the N domain fragments.

Table 2. Mutual positioning of cross-linkers at stop codon nucleotides and amino acid residues of eRF1 in the ribosomal termination complex revealed from the molecular modeling

mRNA analog	Position of the cross-linker site (shown in brackets) with respect to the first nucleotide of the P-site-bound UUC codon	Amino acid residues of eRF1 neighboring N_3 atoms of the cross-linker azide groups[a]
UUC UA*A AAA	+5 (A)	R65, V66
UUC UAA* AAA	+6 (A)	K63-V66
UUC UAA A*AA	+7 (A)	R65, E365
UUC UAAp*	+6 (3′ phosphate)	E104, T362-E367
UUC UAAAp*	+7 (3′ phosphate)	R28, R29, R65, V101-E103, N129
[b]UUC UG*A AAA	+5 (G)	G31–T32, K63, C127, L312–E324, K354–K360
[b]UUC UAG* AAA	+6 (G)	G32–S33, N67–V71, Y125, K354–D359, E370
[b]UUC UAA G*AA	+7 (G)	G31–T32, N67–V71, Y125–K130, K360–H366

[a]To find these amino acid residues, the cross-linkers were added to the respective nucleotides of the mRNA in the models; neighborhood in a 10-Å range was taken into account.
[b]mRNA analogs derivatized at the guanines used in our previous work (24).

This tripeptide is not conserved, but in the majority of organisms the eRF1 position 28 (here and hereafter the human eRF1 numbering is used) is occupied by arginine or lysine (44). Cross-linking of mRNA analogs derivatized at the 3′-phosphates to the 26-AAR-28 region (Table 1) indicates close proximity of this fragment to phosphates on the 3′-side of the UAAA tetraplet. These results provide the first direct experimental data on positioning of the stop signal ribose-phosphate backbone with respect to eRF1 in the 80S termination complex. It is reasonable to suggest that the positively charged side chain of arginine/lysine in eRF1 position 28 interacts with the negatively charged phosphates 3′ of adenosines in the 3rd and 4th positions of the termination tetraplet. Clearly, this interaction cannot mediate discrimination of stop codon purines, but it may contribute to the energy required for the interaction of eRF1 with a stop codon.

A comparison of the results of the present study with data on cross-linking of eRF1 to perfluorophenyl azide-derivatized guanines in stop signals of mRNA analogs (24) reveals two essential differences. First, the 31-GTx-33 motif of eRF1 was the main target for cross-linking with modified guanines of a stop signal (24), but this is not the case for adenines bearing a similar cross-linker (the current study). This provides an indication that positioning of eRF1 toward adenines and guanines of a stop signal in the 80S termination complex is different. The second distinction concerns application of the cross-linking results to data on molecular modeling of the termination complex. Previously (24), a comparison of the results on cross-linking of eRF1 to perfluorophenyl azide-derivatized guanines in stop signals of mRNA analogs with the data of molecular modeling led us to propose the positioning of the stop codon toward eRF1 in the termination complex: only one out of two models (referred as model M1) fitted the cross-linking results. These previous cross-linking results were re-examined with the updated model, in which the GGQ tripeptide of eRF1 is located closer to the CCA terminus of the P-site-bound tRNA, and the same conclusions were reached. In particular, Thr32 from the conserved 31-GTx-33 motif, the major target for cross-linking of the guanine-derivatized mRNA analogs (including the analog with a modified G followed the UAA codon), was present in the set of amino acid residues of eRF1 proximal to stop codon guanines (Table 2). However, in the present study, using the same approach and mRNA analogs bearing a similar cross-linker in the UAAA stop signal, most of the cross-links are not compatible with model M1. No cross-linking of derivatized adenines of UAAA to the eRF1 positions around 63 and/or 65 in the 61-NIKS-64 region is detected (Table 1), and, vice versa, the observed cross-links of adenines in the second, third and fourth stop signal positions to YxCxxxF region (Table 1) are not expected from molecular modeling (Table 2). Only cross-link of the 3′-phosphate of the UAAA tetraplet to Arg28 is anticipated from the model (Table 2). This disagreement can be easily overcome if we suggest that the N domain of eRF1 undergoes a conformational rearrangements leading to a certain displacement of its helices α2 and α3 (Figure 7B, thick dark blue arrows) and of the GT dipeptide (Figure 7B, thick cyan arrow) in opposite directions out of the central axis of the N domain, leaving the arrangements of the Arg28 and YxCxxxF region almost unchanged. These rearrangements allowing the mRNA bases to be placed more deeply in the binding pocket can explain the differences in the eRF1 cross-linking patterns of derivatized stop signal adenines and guanines. In particular, stop signal guanines are recognized by eRF1 in a conformation corresponding to the M1 model (24), whereas recognition of adenines requires eRF1 conformational alterations involving changes of mRNA positioning with respect to the 31-GT-32 dipeptide and helices α2 and α3 that occur easily. The conformation that is preferable for recognition of adenines can be referred as a 'modified pocket conformation'. Deeper dipping of adenines into the eRF1 binding pocket during stop signal recognition may relate to the more hydrophobic nature of adenines as compared to guanines. The modes of purine recognition of stop signals suggested here might provide mechanisms

enabling eRF1 to recognize all three termination signals in contrast to eubacterial class 1 RFs.

The dipeptide GT in positions 31–32 of eRF1 is absolutely conserved in eRF1 and its crucial role in stop codon recognition together with the NIKS and YxCxxxF motifs was predicted (44) and thereafter confirmed experimentally by site-directed mutagenesis (19). Thus, mutation Thr32Ala led to much higher readthrough at both UAA and UAG versus UGA stop codons indicating the importance of this position for the recognition of A in the second stop codon position (19); replacement of the asparagine residue, immediately preceding the GT dipeptide, for His in eRF1 resulted in a reduction of readthrough efficiency with all three stop codons (28). Recently, it has been shown that double substitutions of the non-charged glycine and threonine of the GT dipeptide by the polar and positively charged lysine and arginine in *Euplotes* eRF1b lead to increased readthrough with all three stop codons, confirming the importance of this dipeptide for stop codon recognition (30). It was suggested that hydrogen bonds between Thr32 and Asn67 and between Ser33 and Ser70, together with the sizes and hydrophobicity of Gly31 and Thr32, help to maintain a stable size and orientation of binding pockets for stop codon bases. Cross-linking data make it possible to consider that the GT dipeptide is involved in binding of the stop signal adenine and guanine in different ways. In particular, eRF1 recognizes guanines in a conformation corresponding to model M1 (24) where the GT dipeptide is located close to the guanine and probably directly interacts with it. On the contrary, to recognize adenines, eRF1 changes the conformation of its N domain to adopt a 'modified pocket conformation' so that the GT dipeptide does not interact with the heterocyclic bases of the stop codon, although it remains essential for the maintenance of the local conformation of the N domain suitable for binding of adenines.

There is an additional eRF1 region, aa 70 and 71, implicated in binding/discriminating purines in stop codons. First, the eRF1 mutant Val71Met has been reported to tend toward UAA unipotency (19). This mutation might alter the structure of eRF1 to fix it in a 'modified pocket conformation' preferable for recognition of adenines and complicate the transition to the initial M1 structure that is required for interaction with guanines in stop signals. The importance of a region around position 71 of eRF1 to discriminate purines in stop codons is also followed from recent data demonstrating that the single substitution Ala70Ser in eRF1 of *Euplotes* changes the specificity of the factor from the bipotent UAR specificity to the omnipotent one (29). However, the mechanism whereby this eRF1 region is involved in purine discrimination in stop codons remains unknown. In the X-ray structure of eRF1 complexed with eRF3 (19), Val71 is located close to the bound ATP that is believed to mimic a stop codon. On the other hand, cross-linking data presented earlier (24) and in the current study show that none of the mRNA analogs derivatized at the purine bases of stop codons cross-links to the region surrounding Ser70. The absence of the cross-links itself does not necessarily mean that stop signal purines are not in close proximity to this region since suitable targets for the cross-linker might be lacking. However, probably this suggestion is not applicable to this region because we do observe cross-link in the fragment 67–73 with the mRNA V derivatized at the UAAA 3′-terminal phosphate (Table 1). Therefore, based on the cross-linking data, we suggest that the 70–71 region of eRF1 participates in the interactions maintaining particular N domain conformations responsible for the discrimination of purines in stop codons rather than directly interacts with these purines.

Thus, the data on cross-linking of eRF1 to mRNA analogs derivatized at the guanines of stop signals (24) and at the adenines of the UAAA tetraplet (this study) revealed different positioning of these nucleotides with respect to eRF1 in the 80S termination complexes. The application of the cross-linking results to the structures of eRF1 bound to the ribosome obtained by molecular modeling showed that peptide neighborhoods of guanines and adenines of stop signals are compatible with two alternative conformations of the N domain of eRF1 in the 80S termination complex. The key difference between these conformations of the N domain concerns the positioning of the stop signal purines with respect to the universally conserved dipeptide GT (positions 31–32) in eRF1 that neighbors or even interacts with guanines but is oriented more distantly from adenines. The capability of the ribosome-bound eRF1 to adopt alternative conformations to recognize adenines and guanines without substantial consumption of energy could be essential for recognition of all stop signals by the same class 1 termination factor in eukaryotes. The data obtained give a new insight into the mechanism of stop signal decoding that remains largely unknown due to the lack of cryo-EM and X-ray crystallographic data on 80S termination complexes.

ACKNOWLEDGEMENTS

We gratefully thank Anne-Lise Haenni for critical reading of this manuscript.

FUNDING

The Russian Foundation for Basic Research (grants 11-04-00597 to G.K. and 11-04-00840 to L.F.), and the Program 'Molecular and Cell Biology' of the Presidium of the Russian Academy of Sciences (grants to G.K. and to L.F.). Funding for open access charge: The Program 'Molecular and Cell Biology' of the Presidium of the Russian Academy of Sciences (grant to G.K.).

Conflict of interest statement. None declared.

REFERENCES

1. Nakamura,Y., Ito,K. and Isaksson,L.A. (1996) Emerging understanding of translation termination. *Cell*, **87**, 147–150.
2. Nakamura,Y. and Ito,K. (2003) Making sense of mimic in translation termination. *Trends Biochem. Sci.*, **28**, 99–105.

3. Kisselev,L.L., Ehrenberg,M. and Frolova,LYu. (2003) Termination of translation: interplay of mRNA, rRNAs and release factors. *EMBO J.*, **22**, 175–182.
4. Frolova,L., Le Goff,X., Zhouravleva,G., Davydova,E., Philippe,M. and Kisselev,L. (1996) Eukaryotic polypeptide chain release factor eRF3 is an eRF1- and ribosome-dependent guanosine triphosphatase. *RNA*, **2**, 334–341.
5. Zavialov,A.V., Buckingham,R.H. and Ehrenberg,M. (2001) A posttermination ribosomal complex is the guanine nucleotide exchange factor for peptide release factor RF3. *Cell*, **107**, 115–124.
6. Alkalaeva,E.Z., Pisarev,A.V., Frolova,L.Yu., Kisselev,L.L. and Pestova,T.V. (2006) *In vitro* reconstitution of eukaryotic translation reveals cooperativity between release factors eRF1 and eRF3. *Cell*, **125**, 1125–1136.
7. Salas-Marco,J. and Bedwell,D.M. (2004) GTP hydrolysis by eRF3 facilitates stop codon decoding during eukaryotic translation termination. *Mol. Cell. Biol.*, **24**, 7769–7778.
8. Frolova,L.Y., Simonsen,J.L., Merkulova,T.I., Litvinov,D.Y., Martensen,P.M., Rechinsky,V.O., Camonis,J.H., Kisselev,L.L. and Justesen,J. (1998) Functional expression of eukaryotic polypeptide chain release factors 1 and 3 by means of baculovirus/insect cells and complex formation between the factors. *Eur. J. Biochem.*, **256**, 36–44.
9. Stansfield,I., Jones,K.M., Kushnirov,V.V., Dagkesamanskaya,A.R., Poznyakovski,A.I., Paushkin,S.V., Nierras,C.R., Cox,B.S., Ter-Avanesyan,M.D. and Tuite,M.F. (1995) The products of the SUP45 (eRF1) and SUP35 genes interact to mediate translation termination in *Saccharomyces cerevisiae*. *EMBO J.*, **14**, 4365–4373.
10. Zhouravleva,G., Frolova,L., Le Goff,X., Le Guellec,R., Inge-Vechtomov,S., Kisselev,L. and Philippe,M. (1995) Termination of translation in eukaryotes is governed by two interacting polypeptide chain release factors, eRF1 and eRF3. *EMBO J.*, **14**, 4065–4072.
11. Mitkevich,V.A., Kononenko,A.V., Petrushanko,I.Yu., Yanvarev,D.V., Makarov,A.A. and Kisselev,L.L. (2006) Termination of translation in eukaryotes is mediated by the quaternary eRF1•eRF3•GTP•Mg^{2+} complex. The biological roles of eRF3 and prokaryotic RF3 are profoundly distinct. *Nucleic Acids Res.*, **34**, 3947–3954.
12. Nakamura,Y. and Ito,K. (1998) How protein reads the stop codon and terminates translation. *Genes Cells*, **3**, 265–278.
13. Kisselev,L.L. and Buckingham,R.H. (2000) Translation termination comes of age. *Trends Biochem. Sci.*, **25**, 561–566.
14. Rodnina,M.V. and Wintermeyer,W. (2009) Recent mechanistic insights into eukaryotic ribosomes. *Curr. Opin. Cell. Biol.*, **21**, 435–443.
15. Petry,S., Brodersen,D.E., Murphy,F.V. IV, Dunham,C.M., Selmer,M., Tarry,M.J., Kelley,A.C. and Ramakrishnan,V. (2005) Crystal structures of the ribosome in complex with release factors RF1 and RF2 bound to a cognate stop codon. *Cell*, **123**, 1255–1266.
16. Weixlbaumer,A., Jin,H., Neubauer,C., Voorhees,R.M., Petry,S., Kelley,A.C. and Ramakrishnan,V. (2008) Insights into translational termination from the structure of RF2 bound to the ribosome. *Science*, **322**, 953–956.
17. Korostelev,A., Zhu,J., Asahara,H. and Noller,H.F. (2010) Recognition of the amber UAG stop codon by release factor RF1. *EMBO J.*, **29**, 2577–2585.
18. Song,H., Mugnier,P., Webb,H.M., Evans,D.R., Tuite,M.F., Hemmings,B.A. and Barford,D. (2000) The crystal structure of human eukaryotic release factors eRF1 – mechanism of stop codon recognition and peptidyl-tRNA hydrolysis. *Cell*, **100**, 311–321.
19. Cheng,Z., Saito,K., Pisarev,A.V., Wada,M., Pisareva,V.P., Pestova,T.V., Gajda,M., Round,A., Kong,C., Lim,M. *et al.* (2009) Structural insights into eRF3 and stop codon recognition by eRF1. *Genes Dev.*, **23**, 1106–1118.
20. Ben-Shem,A., Jenner,L., Yusupova,G. and Yusupov,M. (2010) Crystal structure of the eukaryotic ribosome. *Science*, **330**, 1203–1209.
21. Rabl,J., Leibundgut,M., Ataide,S.F., Haag,A. and Ban,N. (2010) Crystal structure of the eukaryotic 40S ribosomal subunit in complex with initiation factor 1. *Science.*, **331**, 730–736.
22. Seit-Nebi,A., Frolova,L. and Kisselev,L. (2002) Conversion of omnipotent translation termination factor eRF1 into ciliate-like UGA-only unipotent eRF1. *EMBO Rep.*, **3**, 881–886.
23. Kolosov,P., Frolova,L., Seit-Nebi,A., Dubovaya,V., Kononenko,A., Oparina,N., Justesen,J., Efimov,A. and Kisselev,L. (2005) Invariant amino acids essential for decoding function of polypeptide release factor eRF1. *Nucleic Acids Res.*, **33**, 6418–6425.
24. Bulygin,K.N., Khairulina,Yu.S., Kolosov,P.M., Ven'yaminova,A.G., Graifer,D.M., Vorobjev,Yu.N., Frolova,L.Yu., Kisselev,L.L. and Karpova,G.G. (2010) Three distinct peptides from the N domain of translation termination factor eRF1 surround stop codon in the ribosome. *RNA*, **16**, 1902–1914.
25. Bertram,G., Bell,H.A., Ritchie,D.W., Fullerton,G. and Stansfield,I. (2000) Terminating eukaryote translation: domain 1 of release factor eRF1 functions in stop codon recognition. *RNA*, **6**, 1236–1247.
26. Lekomtsev,S., Kolosov,P., Bidou,L., Frolova,L., Rousset,J.P. and Kisselev,L. (2007) Different modes of stop codon restriction by the Stylonychia and Paramecium eRF1 translation termination factors. *Proc. Natl Acad. Sci. USA*, **104**, 10824–10829.
27. Fan-Minogue,H., Du,M., Pisarev,A.V., Kallmeyer,A.K., Salas-Marco,J., Keeling,K., Thompson,S.R., Pestova,T. and Bedwell,D.M. (2008) Distinct eRF3 requirements suggest alternate eRF1 conformations mediate peptide release during eukaryotic translation termination. *Mol. Cell.*, **30**, 599–609.
28. Hatin,I., Fabret,C., Rousset,J.P. and Namy,O. (2009) Molecular dissection of translation termination mechanism identifies two new critical regions in eRF1. *Nucleic Acids Res.*, **37**, 1789–1798.
29. Eliseev,B., Kryuchkova,P., Alkalaeva,E. and Frolova,L. (2010) A single amino acid change of translation termination factor eRF1 switches between bipotent and omnipotent stop-codon specificity. *Nucleic Acids Res.*, **39**, 599–608.
30. Wang,Y., Chai,B., Wang,W. and Liang,A. (2010) Functional characterization of polypeptide release factor 1b in the ciliate Euplotes. *Biosci. Rep.*, **30**, 425–431.
31. Chavatte,L., Seit-Nebi,A., Dubovaya,V. and Favre,A. (2002) The invariant uridine of stop codons contacts the conserved NIKSR loop of human eRF1 in the ribosome. *EMBO J.*, **21**, 5302–5311.
32. Matasova,N.B., Myltseva,S.V., Zenkova,M.A., Graifer,D.M., Vladimirov,S.N. and Karpova,G.G. (1991) Isolation of ribosomal subunits containing intact rRNA from human placenta. Estimation of functional activity of 80S ribosomes. *Analyt. Biochem.*, **198**, 219–223.
33. Bulygin,K.N., Repkova,M.N., Ven'yaminova,A.G., Graifer,D.M., Karpova,G.G., Frolova,L.Yu. and Kisselev,L.L. (2002) Positioning of the mRNA stop signal with respect to polypeptide chain release factors and ribosomal proteins in 80S ribosomes. *FEBS Lett.*, **514**, 96–101.
34. Repkova,M.N., Ivanova,T.M., Komarova,N.I., Meschaninova,M.I., Kuznetsova,M.A. and Ven'yaminova,A.G. (1999) *H*-Phosphonate synthesis of oligoribonucleotides containing modified bases. I. Photoactivatable derivatives of oligoribonucleotides with perfluoroarylazide groups in heterocyclic bases. *Russ. J. Bioorg. Chem.*, **25**, 612–622.
35. Smolenskaya,I.A., Bulygin,K.N., Graifer,D.M., Ivanov,A.V., Ven'yaminova,A.G., Repkova,M.N. and Karpova,G.G. (1998) Localization of template in the decoding area by affinity modification of human ribosomes with photoactivated derivative of oligoribonucleotide pGUGUUU. *Mol. Biol.*, **32**, 233–241.
36. Frolova,L., Seit-Nebi,A. and Kisselev,L. (2002) Highly conserved NIKS tetrapeptide is functionally essential in eukaryotic translation termination factor eRF1. *RNA*, **8**, 129–136.
37. Frolova,L.Y., Merkulova,T.I. and Kisselev,L.L. (2000) Translation termination in eukaryotes: polypeptide release factor eRF1 is composed of functionally and structurally distinct domains. *RNA*, **6**, 381–390.
38. Caskey,C., Beaudet,A.L. and Tate,W.P. (1974) Mammalian release factor: in vitro assay and purification. *Methods Enzymol.*, **30**, 293–303.

39. Frolova,L., Le Goff,X., Rasmussen,H.H., Cheperegin,S., Drugeon,G., Kress,M., Arman,I., Haenni,A.-L., Celis,J.E., Philippe,M. *et al*. (1994) A highly conserved eukaryotic protein family possessing properties of polypeptide chain release factor. *Nature*, **372**, 701–703.
40. Graifer,D., Molotkov,M., Styazhkina,V., Demeshkina,N., Bulygin,K., Eremina,A., Ivanov,A., Laletina,E., Ven'yaminova,A. and Karpova,G. (2004) Variable and conserved elements of human ribosomes surrounding the mRNA at the decoding and upstream sites. *Nuceic Acids Res*., **32**, 3282–3293.
41. Molotkov,M., Graifer,D., Demeshkina,N., Repkova,M., Ven'yaminova,A. and Karpova,G. (2005) Arrangement of mRNA 3′ of the A site codon on the human 80S ribosome. *RNA Biol*., **2**, 63–69.
42. Mantsyzov,A.B., Ivanova,E.V., Birdsall,B., Alkalaeva,E.Z., Kryuchkova,P.N., Kelly,G., Frolova,L.Y. and Polshakov,V.I. (2010) NMR solution structure and function of the C-terminal domain of eukaryotic class1 polypeptide chain release factor. *FEBS J*., **277**, 2611–2627.
43. Pisarev,A.V., Kolupaeva,V.G., Yusupov,M.M., Hellen,C.U.T. and Pestova,T.V. (2008) Ribosomal position and contacts of mRNA in eukaryotic translation initiation complexes. *EMBO J*., **27**, 1609–1621.
44. Liang,H., Wong,J.Y., Bao,Q., Cavalcanti,A.R.O. and Landweber,L.F. (2005) Decoding region: analysis of eukaryotic release factor (eRF1) stop codon binding residues. *J. Mol. Evol*., **60**, 337–344.